Available online at www.sciencedirect.com

jmr&t
Journal of Materials Research and Technology

journal homepage: www.elsevier.com/locate/jmrt

Original Article

Navigating viscosity of ferrofluid using response surface methodology and artificial neural network

Nidal H. Abu-Hamdeh [a], *Ali Golmohammadzadeh* [b], *Aliakbar Karimipour* [c,*]

[a] Center of Research Excellence in Renewable Energy and Power Systems, And Department of Mechanical Engineering, Faculty of Engineering, King Abdulaziz University, Jeddah 21589, Saudi Arabia
[b] Sapienza Università di Roma, Via Eudossiana 18, Roma, 00184, Italy
[c] Institute of Research and Development, Duy Tan University, Da Nang 550000, Vietnam

* Corresponding author.
E-mail addresses: nabuhamdeh@kau.edu.sa (N.H. Abu-Hamdeh), aliakbarkarimipour@duytan.edu.vn (A. Karimipour).
* Corresponding author.
E-mail addresses: nabuhamdeh@kau.edu.sa (N.H. Abu-Hamdeh), aliakbarkarimipour@duytan.edu.vn (A. Karimipour).
* Corresponding author.
E-mail addresses: nabuhamdeh@kau.edu.sa (N.H. Abu-Hamdeh), aliakbarkarimipour@duytan.edu.vn (A. Karimipour).
* Corresponding author.
E-mail addresses: nabuhamdeh@kau.edu.sa (N.H. Abu-Hamdeh), aliakbarkarimipour@duytan.edu.vn (A. Karimipour).
* Corresponding author.
E-mail addresses: nabuhamdeh@kau.edu.sa (N.H. Abu-Hamdeh), aliakbarkarimipour@duytan.edu.vn (A. Karimipour).
* Corresponding author.
E-mail addresses: nabuhamdeh@kau.edu.sa (N.H. Abu-Hamdeh), aliakbarkarimipour@duytan.edu.vn (A. Karimipour).
* Corresponding author.
E-mail addresses: nabuhamdeh@kau.edu.sa (N.H. Abu-Hamdeh), aliakbarkarimipour@duytan.edu.vn (A. Karimipour).
* Corresponding author.
E-mail addresses: nabuhamdeh@kau.edu.sa (N.H. Abu-Hamdeh), aliakbarkarimipour@duytan.edu.vn (A. Karimipour).
* Corresponding author.
E-mail addresses: nabuhamdeh@kau.edu.sa (N.H. Abu-Hamdeh), aliakbarkarimipour@duytan.edu.vn (A. Karimipour).
* Corresponding author.
E-mail addresses: nabuhamdeh@kau.edu.sa (N.H. Abu-Hamdeh), aliakbarkarimipour@duytan.edu.vn (A. Karimipour).
* Corresponding author.
E-mail addresses: nabuhamdeh@kau.edu.sa (N.H. Abu-Hamdeh), aliakbarkarimipour@duytan.edu.vn (A. Karimipour).
* Corresponding author.
E-mail addresses: nabuhamdeh@kau.edu.sa (N.H. Abu-Hamdeh), aliakbarkarimipour@duytan.edu.vn (A. Karimipour).
* Corresponding author.
E-mail addresses: nabuhamdeh@kau.edu.sa (N.H. Abu-Hamdeh), aliakbarkarimipour@duytan.edu.vn (A. Karimipour).
https://doi.org/10.1016/j.jmrt.2020.11.087

Nomenclature

k	*Thermal Conductivity* $Wm^{-1}K^{-1}$
MF	*Mass fraction*
TCR	*Thermal conductivity ratio* $\left(\frac{k_{nf}}{k_{bf}}\right)$
T	*Temperature* (°C)
VF	*Volume fraction*
RSM	*Response surface methodology*

Greek Letters

μ	*Viscosity* (*mPa.s*)
$\dot{\gamma}$	*Shear rate*

ARTICLE INFO

Article history:
Received 10 September 2020
Accepted 24 November 2020
Available online 1 December 2020

Keywords:
Ferrofluid
ANN
RSM
Thermal Conductivity

ABSTRACT

The main purpose of this study is to investigate the capabilities of artificial neural network (ANN) and response surface methodology (RSM) in estimating the viscosity of Fe_3O_4 nanofluid. Nanoparticles increase the resistance to motion and thus boost the viscosity. Initially, the rheological behavior of the base fluid and nanofluid was investigated and it was found that both fluids are not particularly sensitive to the shear rate, which indicates the Newtonian behavior. Input parameters of temperature and volume fraction and output parameter, nanofluid viscosity were introduced to both techniques to find the best correlation in which the viscosity can be predictable. Comparison of R-square in ANN (0.999) and RSM (0.996) techniques showed that both techniques can navigate the viscosity well. Also the margin of deviation (MOD) and mean square error (MSE) for ANN were 4.22% and 0.0000741 which were lower than the corresponding values in RSM one (MOD = 5.52%, MSE = 0.00027).

1. Introduction

Reducing energy consumption is a critical issue for human activity on Earth, and has attracted the attention of many researchers in building [1–7], solar still [8–12] and solar applications [13–16]. One of the techniques to reduce consumption can be met by non-materials. The presence of nanoparticles in fluids dates back to the 20th century. Since then, many studies have been conducted in which researchers [5,17–23] have prepared many samples of nanofluids to improve the performance of various devices [12,24–28]. Because mathematics [5,29] is used in many sciences [29,30], artificial intelligence-based [31,32] techniques can also be used to reduce the number of experiments. Tian et al. [33] applied ANN on Gr/EG to investigate the nanofluid surface tension. They tested nanofluid samples prepared in 0.005–5 wt.% to measure surface tension at 25–70°C. Also, they developed a neural network consisting of three layers. The input layer included two neurons, which were assigned to the T and WF, and for the output layer, only one neuron was considered for surface tension. The number of neurons in the middle layer was not reported by the authors. A comparison between $(\sigma_{Gr/EG})_{Exp}$ and $(\sigma_{Gr/EG})_{Pred}$ showed that MOD was less than 1.5%. From the perspective of ANN accuracy, it was affirmed that the R^2 and *MSE* values were equal to 0.986 and 5.068×10^{-8}, respectively. Li et al. [34] attempted to predict the $k_{Al_2O_3/EG}$ and $\mu_{Al_2O_3/EG}$ using a neural network and then evaluate the accuracy of the method by comparing it with experimental results. It was found that the coefficient of determination for viscosity and conductivity was $(R^2)_{\mu} = 0.9984$ and $(R^2)_{k} = 0.9997$, respectively.

Yan et al. [35] prepared samples of MWCNT/liquid paraffin and then investigated the nanofluids behavior by measuring $\sigma_{MWCNT/Paraffin}$. The two neurons that created the input layer were assigned to T and MF while in the output layer one neurons was assigned to surface tension. The authors found that three neurons were appropriate for the middle layer. Comparisons between $(\sigma_{MWCNT/Paraffin})_{Exp}$ and $(\sigma_{MWCNT/Paraffin})_{Pred}$ revealed that the values of R^2 and *MSE* and *MOD* were 0.997, 5.568×10^{-6} and 0.998%, respectively. Akhgar et al. [36] inserted TiO_2 and MWCNT (50:50) into EG-water (50:50 vol.%) and measured k_{nf} at 25–50°C. The neurons in the first, second, and third layers were two, four, and one, respectively. A comparison between $(k_{TiO_2+MWCNT/w+EG})_{Exp}$ and $(k_{TiO_2+MWCNT/w+EG})_{Pred}$ revealed that the MOD of the developed ANN was less than 2.1%. In another study, Ma et al. [37] evaluated the ability of the ANN method for prediction of viscosity and thermal conductivity of Al_2O_3–CuO/Water-EG. They measured the accuracy of the ANN technique by calculating the coefficient of determination and revealed that this parameter for μ and k

was $(R^2)_{\mu} = 0.9755$ and $(R^2)_{k} = 0.9846$. Li et al. [38] prepared MgO/water nanofluid at 0.07–1.25 vol.% and measured viscosity at 25–60°C. The neural network developed by the authors to predict $\mu_{MgO/Water}$ consisted of 3 layers. Three neurons were added to the first layer to cover the input variables of *T*, *VF* and $\dot{\gamma}$ while in the output layer, only one neuron was allocated for viscosity. The use of trial and error have shown that 24 neurons are the most suitable model for the middle layer. Authors reported that the developed ANN has the values of 0.999 and 0.0118 for R^2 and *MSE*, respectively. Ghazvini et al. [39] found that $k_{CuFe_2O_4/water}$ was predictable by the use of ANN method at 10–70°C and 0–14 wt.%. By assigning two neurons in the input layer to *T* and *MF*, one neuron for $k_{CuFe_2O_4/water}$, and an optimal number equal to six neurons for the middle layer, they showed that the ability of the ANN method is very high so that the values of 2.5×10^{-4} and 0.97 were obtained for *MSE* and R^2, respectively. Similar to [39], a study conducted by Esfe and Motallebi [40] investigated the appropriateness of using the ANN method to estimate $k_{Al/oil}$, $\mu_{Al/oil}$ and $c_{p\,Al/oil}$. A comparison was made between the experimental and predicted data and showed that all three parameters, taking into account values of $R^2_k = 0.99$, $R^2_{\mu} = 0.846$ and $R^2_{c_p} = 0.895$, could well be estimated by ANN methodology.

The response surface methodology (RSM) method has also been evaluated by various researchers [41] and their results show that this method is very simple and at the same time, has acceptable accuracy. Esfe et al. [42] applied RSM to predict the $\frac{k_{Al_2O_3/water}}{k_{water}}$ as well as $\frac{\mu_{Al_2O_3/water}}{\mu_{water}}$ at 300–325K and 1–5 vol.%. through performing regression criteria, it was found that the coefficient of determination were $(R^2)_{\frac{k_{Al_2O_3/water}}{k_{water}}} = 0.9997$ and $(R^2)_{\frac{\mu_{Al_2O_3/water}}{\mu_{water}}} = 0.9955$. In addition, they approved RSM for the nanofluid of CuO/water and observed that the values of $(R^2)_{\frac{k_{CuO/water}}{k_{water}}}$ and $(R^2)_{\frac{\mu_{CuO/water}}{\mu_{water}}}$ were 0.9996 and 0.9956 respectively. Tian et al. [43] applied RSM to predict the $\frac{k_{Al2O3-MWCNT/10w40}}{k_{10w40}}$ at 0.05–1 vol.% and 25–65°C. Performing regression criteria, it

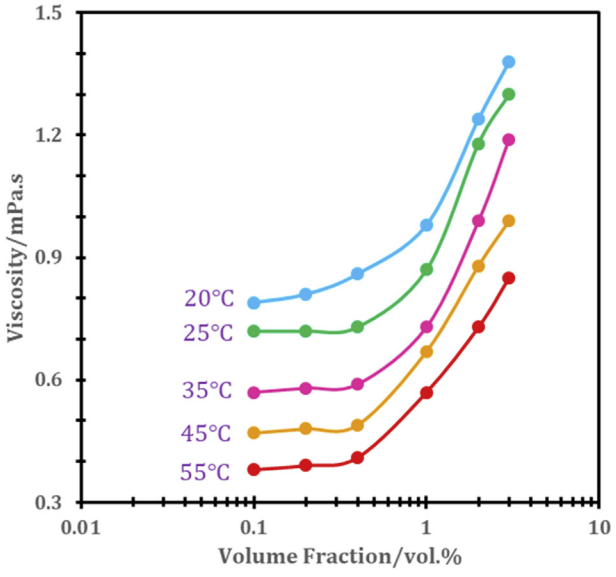

Fig. 1 – Measured viscosity [51].

Table 1 – ANOVA outputs.

Parameter	F -value	P -value
T	150	<0.0001
ϕ	500	<0.0001
Tϕ	28	<0.0001
T^2	9.4	0.0051
ϕ^2	11	0.003
$T^2\phi$	10	0.0038
$T\phi^2$	0.94	0.34
T^3	2	0.17
ϕ^3	27	<0.0001

was found that the values of R^2, *MSE* and MOD_{max} were 0.9948, 0.0008485 and 0.97%, respectively. Yan et al. [41] also examined RSM for the prediction of $\mu_{MWCNTs-TiO2/EG}$ at 25–55°C. The ability of the RSM method was excellent because the values of R^2, *MSE* and MOD_{max} were 0.995, 0.00418 and 9.54%, respectively.

When ferrofluids [44–46] are exposed to a magnetic field, they exhibit magnetic properties that are used in the medical and aerospace industries and have been studied by many researchers [47–50]. In this investigation, the viscosity of Fe3O4/water nanofluid is predicted by using ANN and RSM techniques. In both techniques, considering the lowest R-square criteria, the suitable continuous function and appropriate neuron numbers are extracted. Moreover, mean square error and margin of deviation for both techniques will be calculated. Finally, through performing a comparison, the accuracy of ANN and RSM are evaluated.

2. Reference data

In both cases, the input information must be introduced into the system. The input information in this study was the Fe3O4/water viscosity, which was measured experimentally by Toghraie et al. [51] The authors observed that the viscosity did not depend to the shear rate. The input variables were limited to *T* and ϕ within the range of 20–55°C and 0.1–3 vol.%, respectively. Fig. 1 shows the amount of viscosity measured in the laboratory.

3. RSM technique

As mentioned in the RSM technique, a function is utilized to estimate the value of the objective parameter. This function is a set of several linear expressions [52]. In this study, the inputs include *T* and ϕ and therefore, for the cubic models, the fitted function includes main factors such as T, ϕ, T^2, ϕ^2, T^3, ϕ^3 and interaction factors such as Tϕ, $T^2\phi$ and $T\phi^2$. Each factor affects

Table 2 – Coefficients value of the proposed correlation.

Parameter	Value	Parameter	Value
a_0	1.4	a_5	0.13
a_1	−0.045	a_6	−8 E−5
a_2	0.015	a_7	−0.00031
a_3	0.0056	a_8	−4.3 E−6
a_4	0.0007	a_9	−0.029

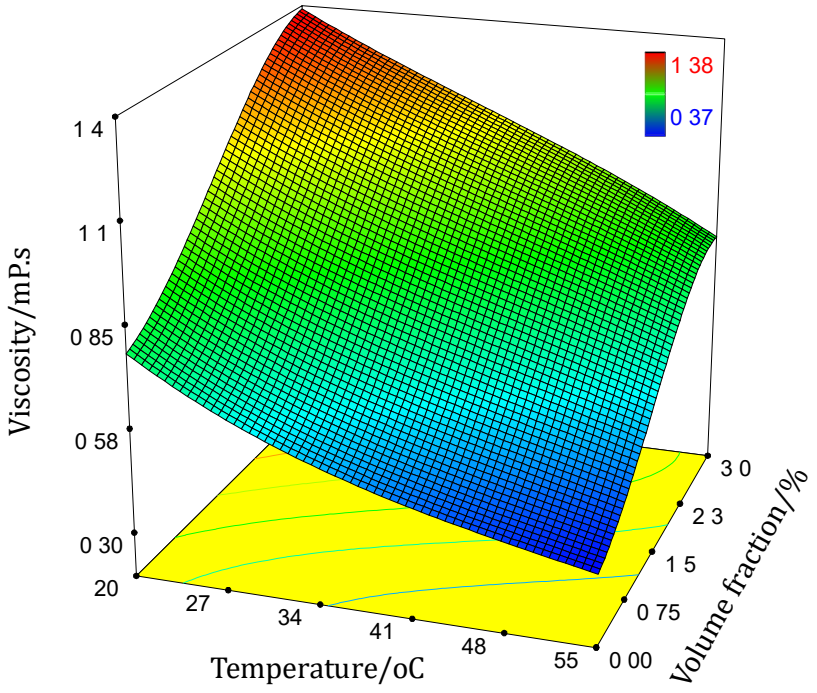

Fig. 2 – Predicted viscosity in terms of T and ϕ.

the output function. In other words, each factor is multiplied by a constant coefficient, and by summing all of them, the output function is extracted. The importance of each factor is determined by the P-value test and based on the P-value test criteria, for $P > 0.1$, it can be claimed that the factor does not have a significant effect on the objective function. The constant-coefficient value is determined by ANOVA and using the least-square method. Note that, in this technique, in addition to cubic models, there are also square and linear

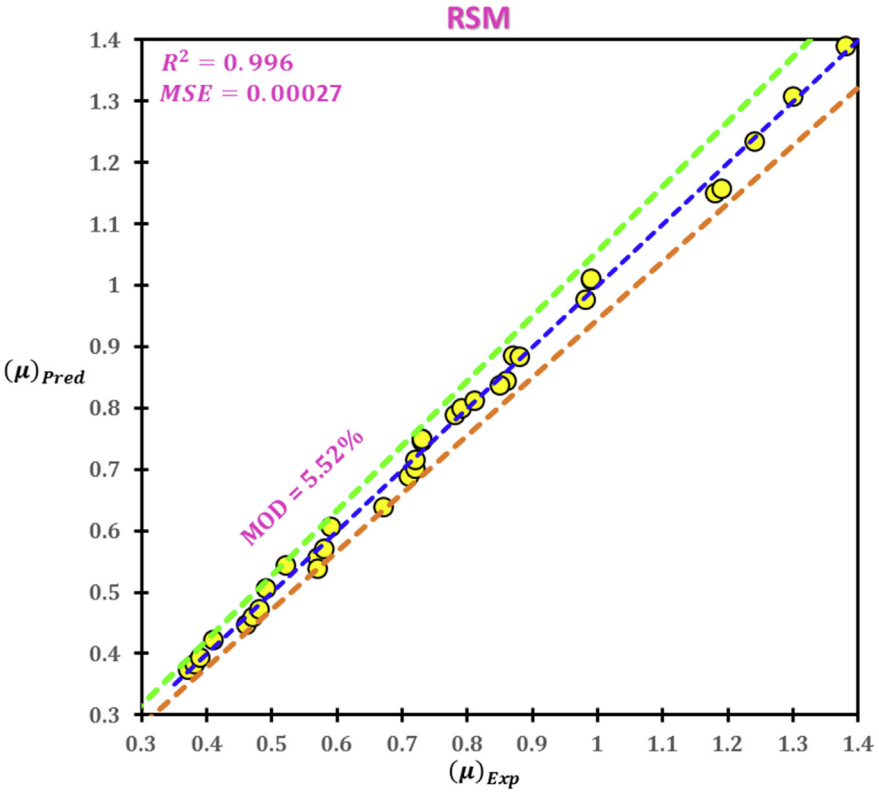

Fig. 3 – Predicted versus experimental viscosity (RSM).

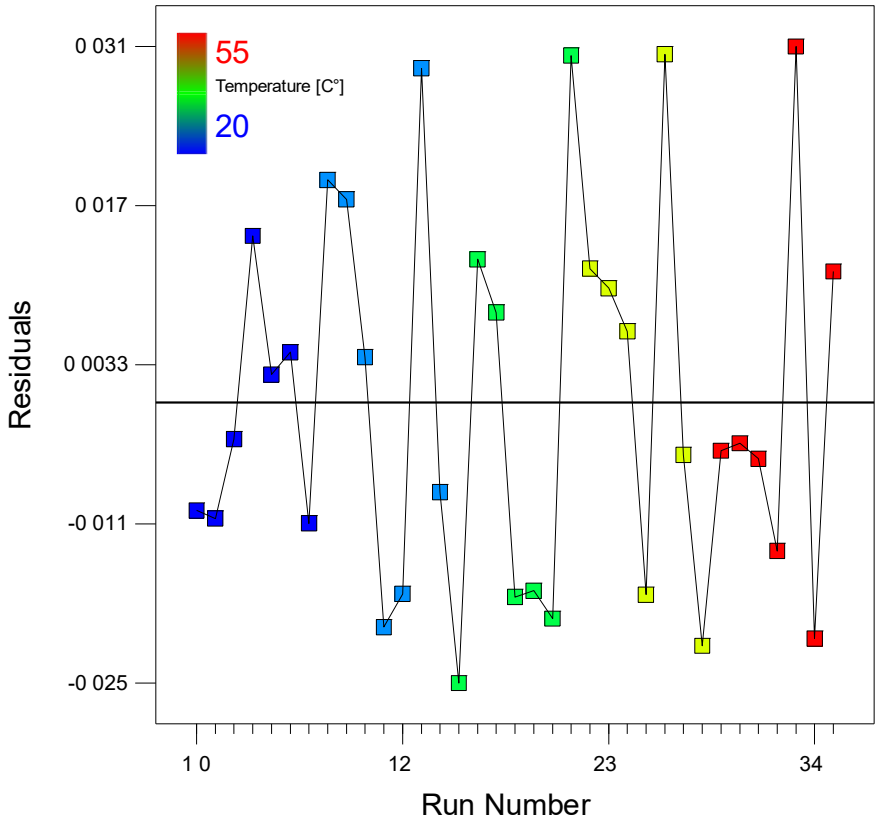

Fig. 4 – Residuals at different temperature.

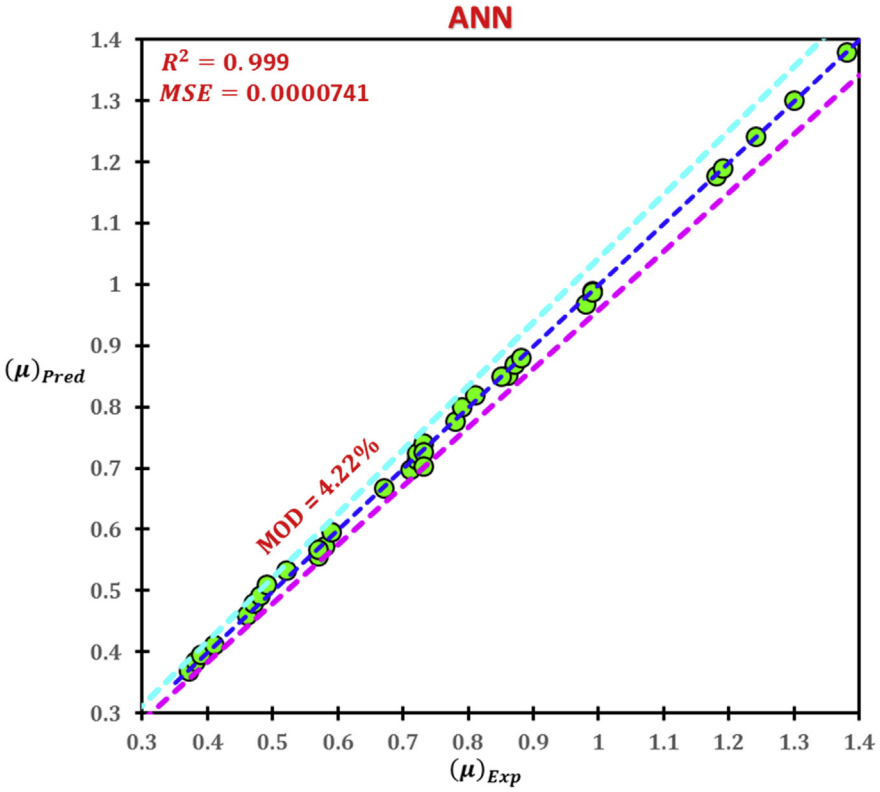

Fig. 5 – Predicted versus experimental viscosity (ANN).

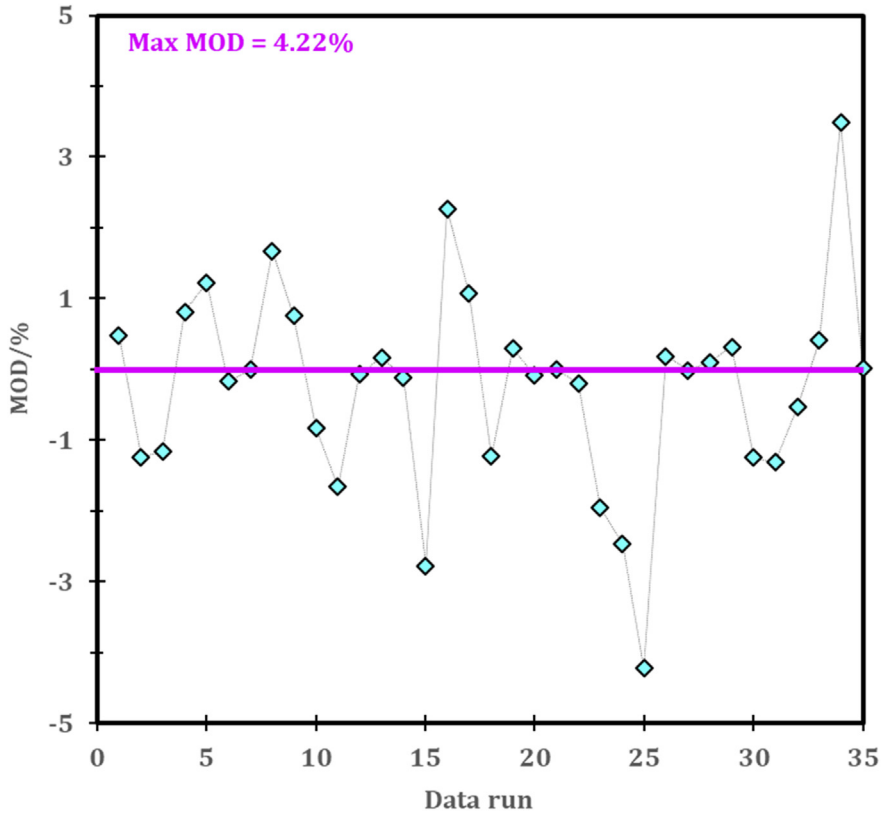

Fig. 6 – Margin of deviation for the ANN technique.

models. In the square model, the total power of each factor should not be less than two.

4. ANN

In the artificial neural network technique, the input information is utilized to find the output variables after passing through three layers. In ANN, the value of the output parameter is generated at the discrete points [53]. In this technique, the input information is divided into three parts: training, validation and test. In this study, the total number of input data was 35 and for training, validation and test sections, 25, 5 and 5 points were assigned, respectively. The accuracy of the neural network depends on the number of neurons in the middle layer, and in general, there is no correlation to obtain the optimal neurons number, and it should be referred to methods based on trial and error.

Table 3 – Comparison of the statistical criterion for ANN and RSM.

	R^2	MSE	MOD_{max}
ANN	0.999	0.0000741	4.22%
RSM	0.996	0.00027	5.52%

5. Results

The main purpose of this paper is to investigate the accuracy of RSM and ANN methods in estimating $\mu_{Fe_3O_4/water}$. Therefore, first, the results of each technique are mentioned separately and then they are compared.

5.1. *RSM outputs*

In the regression technique [54,55], it is always tried to predict the effects of independent variables on the dependent ones using a function (linear or nonlinear). The RSM method focuses on several polynomials functions. The polynomials function used in the RSM technique are limited to first, second, and third polynomials. By implementing the statistical calculation, R-squared value for the linear, quadratic and cubic polynomial is 0.98, 0.991 and 0.996 respectively. This implies that the cubic model has priority to other ones. By implementing the analysis of variance (ANOVA), each parameter importance is determined. The results of ANOVA summarized in Table 1.

Finally, the following cubic polynomial correlation is derived:

$$\mu_{nf} = a_0 + a_1\, T + a_2\, \phi + a_3 T\phi + a_4\, T^2 + a_5\, \phi^2 + a_6\, T^2\phi + a_7\, T\phi^2 + a_8\, T^3 + a_9\phi^3 \quad (1)$$

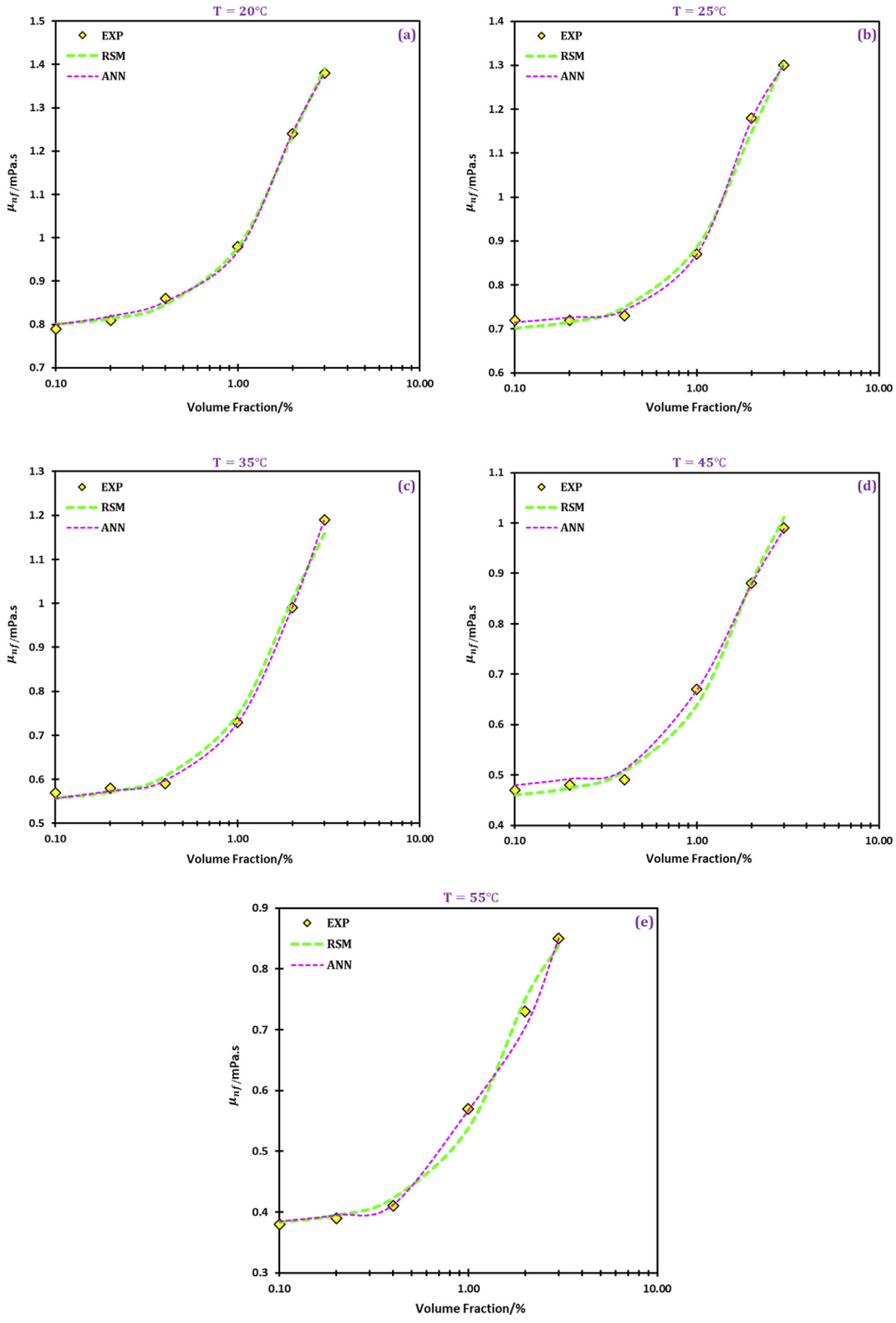

Fig. 7 – Comparison of ANN and RSM techniques.

The coefficients of the proposed correlation are reported in Table 2.

Fig. 2 shows the amount of viscosity in terms of ϕT and ϕ. The maximum viscosity value is 1.38 mPa s, which is subject to conditions $T = 20^{\circ}C$ and. $\phi = 3$ vol.%

Fig. 3 shows the correlation between $\mu_{Epx}$and μ_{Pred}parameters. Under the best conditions, if all points are on the bisector line, the correlation accuracy is at its maximum value, in which case the parameters of R^2, MSE and $MOD_{max}$are unity, zero and 0%, respectively. However, Eq. (1) is a correlation based on the minimal squares method, which means that there is a small error in viscosity estimation. Owing to error, the parameters of R^2, MSE and $MOD_{max}$are 0.996, 0.00027 and 5.52%, respectively.

The error value (residual) for Eq. (1) is obtained by subtracting the value of the experimental viscosity and the estimated viscosity. Fig. 4 shows the residual of the total reference data. The maximum residual value is within the range of −0.025 mPa s to 0.031 mPa s.

5.2. *ANN results*

The developed neural network in the input and output layers has two and one neurons, respectively, but since the number of neurons in the middle layer is not known, the most appropriate number of neurons must be obtained by repetition. In this study, the most appropriate number of neurons in the middle layer is ten. In total, the neural network consisting of 13 neurons (two neurons in the input layer, ten neurons in the middle layer, and one neuron in the output layer) is able to navigate the behavior of Fe3O4/water from a viscosity perspective. As mentioned in the RSM technique, Fig. 5 is used to examine the correspondence between the experimental and predicted data. There is a very high match between the numerical results and experimental ones. However, to ensure the strength of the ANN, the values of R^2 and MSE for this network are calculated and the results are shown in Fig. 5.

Margin of deviation (MOD) for each experimental data can be seen in Fig. 6. As shown in Fig. 6, in just four points, the MOD value is greater than 2%. Elsewhere, MOD value are less than 2%. However, the maximum MOD was calculated to be 4.22%.

5.3. *Comparison of ANN and RSM*

In this section, the ability of both methods to estimate $\mu_{Fe_3O_4/water}$nanofluid is compared. The comparison of the two techniques from the statistical perspective is reported in Table 3.

The ANN method has a higher R-squared value as well as lower MSE and MOD which implies that using ANN is superior to the RSM technique. The second method of comparison is to illustrate laboratory data and output techniques. In Fig. 7, at each temperature, a comparison is performed with respect to the mass fraction, so that the accuracy of both techniques is well illustrated.

As shown in Fig. 7, both techniques are highly accurate. However, the strength of the ANN is slightly better than the RSM technique especially at higher temperatures.

6. conclusion

In this research, $\mu_{Fe_3O_4/water}$ was investigated numerically. For numerical study, RSM and ANN techniques were used, and by applying the least-square technique, the best polynomials and the most appropriate number of neurons in the middle layer were identified. The main findings were:

* Considering the amount of R^2in ANN (0.999) and RSM (0.996), it can be said that from this perspective, the neural network is better.
* The value of MSE in the ANN (0.0000741) and RSM (0.00027) indicates that the amount of error in the RSM technique is more than ANN one.
* The maximum margin of deviation for the neural network (4.22%) and RSM (5.52%) technique also indicates that the neural network is stronger than RSM by considering this criterion.
* Comparison between the neural network and RSM trend, affirmed the superiority of the neural network.

Finally, it can be concluded that the ANN method compared to the RSM technique is superior.

Declaration of Competing Interest

There is no conflict of interest.

Acknowledgment

The Deanship of Scientific Research (DSR) at King Abdulaziz University, Jeddah, Saudi Arabia funded this project, under grant no. (FP-202-42).

REFERENCES

[1] Liu W, Kalbasi R, Afrand M. Solutions for enhancement of energy and exergy efficiencies in air handling units. J Clean Prod 2020;257:120565. https://doi.org/10.1016/j.jclepro.2020.120565.

[2] Mallikarjuna K, Santhoshkumar Reddy Y, Hemachandra Reddy K, Sanjeeva Kumar PV. A nanofluids and nanocoatings used for solar energy harvesting and heat transfer applications: a retrospective review analysis. Mater Today: Proc 2020. https://doi.org/10.1016/j.matpr.2020.05.833 [in press].

[3] Yurddaş A. Optimization and thermal performance of evacuated tube solar collector with various nanofluids. Int J Heat Mass Tran 2020;152:119496. https://doi.org/10.1016/j.ijheatmasstransfer.2020.119496.

[4] Shahsavar Goldanlou A, Kalbasi R, Afrand M. Energy usage reduction in an air handling unit by incorporating two heat recovery units. J Build Eng 2020;32:101545. https://doi.org/10.1016/j.jobe.2020.101545.

[5] Kalbasi R, Ruhani B, Rostami S. Energetic analysis of an air handling unit combined with enthalpy air-to-air heat exchanger. J Therm Anal Calorim 2020;139(4):2881–90. https://doi.org/10.1007/s10973-019-09158-9.

[6] Kalbasi R, Shahsavar A, Afrand M. Reducing AHU energy consumption by a new layout of using heat recovery units. J Therm Anal Calorim 2020;139(4):2811–20. https://doi.org/10.1007/s10973-019-09070-2.
[7] Alsagri AS, Arabkoohsar A, Khosravi M, Alrobaian AA. Efficient and cost-effective district heating system with decentralized heat storage units, and triple-pipes. Energy 2019;188:116035.
[8] Parsa SM, Javadi YD, Rahbar A, Majidniya M, Aberoumand S, Amidpour Y, et al. Experimental assessment on passive solar distillation system on Mount Tochal at the height of 3964m: Study at high altitude. Desalination 2019;466:77–88. https://doi.org/10.1016/j.desal.2019.05.010.
[9] Parsa SM, Javadi YD, Rahbar A, Majidniya M, Salimi M, Amidpour Y, et al. Experimental investigation at a summit above 13,000ft on active solar still water purification powered by photovoltaic: a comparative study. Desalination 2020;476:114146. https://doi.org/10.1016/j.desal.2019.114146.
[10] Parsa SM, Rahbar A, Javadi Y D, Koleini MH, Afrand M, Amidpour M. Energy-matrices, exergy, economic, environmental, exergoeconomic, enviroeconomic, and heat transfer (6E/HT) analysis of two passive/active solar still water desalination nearly 4000m: altitude concept. J Clean Prod 2020;261:121243. https://doi.org/10.1016/j.jclepro.2020.121243.
[11] Parsa SM, Rahbar A, Koleini MH, Aberoumand S, Afrand M, Amidpour M. A renewable energy-driven thermoelectric-utilized solar still with external condenser loaded by silver/nanofluid for simultaneously water disinfection and desalination. Desalination 2020;480:114354. https://doi.org/10.1016/j.desal.2020.114354.
[12] Parsa SM, Rahbar A, Koleini MH, Javadi YD, Afrand M, Rostami S, et al. First approach on nanofluid-based solar still in high altitude for water desalination and solar water disinfection (SODIS). Desalination 2020;491:114592. https://doi.org/10.1016/j.desal.2020.114592.
[13] Alsagri AS. Design and dynamic simulation of a photovoltaic thermal-organic Rankine cycle considering heat transfer between components. Energy Convers Manag 2020;225:113435.
[14] Alsagri AS. Energy performance enhancement of solar thermal power plants by solar parabolic trough collectors and evacuated tube collectors-based preheating units. Int J Energy Res 2020;44(8):6828–42.
[15] Alsagri AS, Arabkoohsar A, Alrobaian AA. Combination of subcooled compressed air energy storage system with an Organic Rankine Cycle for better electricity efficiency, a thermodynamic analysis. J Clean Prod 2019;239:118119.
[16] Mohammed RH, Alsagri AS, Wang X. Performance improvement of supercritical carbon dioxide power cycles through its integration with bottoming heat recovery cycles and advanced heat exchanger design: a review. Int J Energy Res 2020;44(9):7108–35.
[17] Kazemi I, Sefid M, Afrand M. Improving the thermal conductivity of water by adding mono & hybrid nano-additives containing graphene and silica: a comparative experimental study. Int Commun Heat Mass Tran 2020;116:104648. https://doi.org/10.1016/j.icheatmasstransfer.2020.104648.
[18] Wei H, Afrand M, Kalbasi R, Ali HM, Heidarshenas B, Rostami S. The effect of tungsten trioxide nanoparticles on the thermal conductivity of ethylene glycol under different sonication durations: an experimental examination. Powder Technol 2020;374:462–9. https://doi.org/10.1016/j.powtec.2020.07.056.
[19] Kazemi I, Sefid M, Afrand M. A novel comparative experimental study on rheological behavior of mono & hybrid nanofluids concerned graphene and silica nano-powders: characterization, stability and viscosity measurements. Powder Technol 2020;366:216–29. https://doi.org/10.1016/j.powtec.2020.02.010.
[20] Bashiri Rezaie A, Montazer M. Shape-stable thermo-responsive nano Fe3O4/fatty acids/PET composite phase-change material for thermal energy management and saving applications. Appl Energy 2020;262:114501. https://doi.org/10.1016/j.apenergy.2020.114501.
[21] Rostami S, Kalbasi R, Sina N, Goldanlou AS. Forecasting the thermal conductivity of a nanofluid using artificial neural networks. J Therm Anal Calorim 2020. https://doi.org/10.1007/s10973-020-10183-2.
[22] Afrand M. Experimental study on thermal conductivity of ethylene glycol containing hybrid nano-additives and development of a new correlation. Appl Therm Eng 2017;110:1111–9. https://doi.org/10.1016/j.applthermaleng.2016.09.024.
[23] Kalbasi R, Izadi F, Talebizadehsardari P. Improving performance of AHU using exhaust air potential by applying exergy analysis. J Therm Anal Calorim 2020;139(4):2913–23. https://doi.org/10.1007/s10973-019-09198-1.
[24] Yan S-R, Kalbasi R, Karimipour A, Afrand M. Improving the thermal conductivity of paraffin by incorporating MWCNTs nanoparticles. J Therm Anal Calorim 2020. https://doi.org/10.1007/s10973-020-09819-0.
[25] Rostami S, Afrand M, Shahsavar A, Sheikholeslami M, Kalbasi R, Aghakhani S, et al. A review of melting and freezing processes of PCM/Nano-PCM and their application in energy storage. Energy 2020:118698. https://doi.org/10.1016/j.energy.2020.118698.
[26] Dehkordi KG, Karimipour A, Afrand M, Toghraie D, Isfahani AHM. Molecular dynamics simulation concerning nanofluid boiling phenomenon affected by the external electric field: effects of number of nanoparticles through Pt, Fe, and Au microchannels. J Mol Liq 2020:114775. https://doi.org/10.1016/j.molliq.2020.114775.
[27] Raisi A, Rostami S, Nadooshan AA, Afrand M. The examination of circular and elliptical vanes under natural convection of nanofluid in a square chamber subject to radiation effects. Int Commun Heat Mass Tran 2020;117:104770. https://doi.org/10.1016/j.icheatmasstransfer.2020.104770.
[28] Yan S-R, Izadi M, Sheremet MA, Pop I, Oztop HF, Afrand M. Inclined Lorentz force impact on convective-radiative heat exchange of micropolar nanofluid inside a porous enclosure with tilted elliptical heater. Int Commun Heat Mass Tran 2020;117:104762. https://doi.org/10.1016/j.icheatmasstransfer.2020.104762.
[29] Afrand M, Kalbasi R, Karimipour A, Wongwises S. Experimental investigation on a thermal model for a basin solar still with an external reflector. Energies 2017;10(1):18.
[30] Mosavi A, Mehdizadeh H, Abbasian-Naghneh S, Kalbasi R, Karimipour A, Cheraghian G. Incorporation of horizontal fins into a PCM-based heat sink to enhance the safe operation time: applicable in electronic device cooling. Appl Sci 2020;10(18):6308 [Online]. Available: https://www.mdpi.com/2076-3417/10/18/6308.
[31] Rostamian SH, Biglari M, Saedodin S, Hemmat Esfe M. An inspection of thermal conductivity of CuO-SWCNTs hybrid nanofluid versus temperature and concentration using experimental data, ANN modeling and new correlation. J Mol Liq 2017;231:364–9. https://doi.org/10.1016/j.molliq.2017.02.015.
[32] Hemmat Esfe M, Esfandeh S, Saedodin S, Rostamian H. Experimental evaluation, sensitivity analyzation and ANN modeling of thermal conductivity of ZnO-MWCNT/EG-water hybrid nanofluid for engineering applications. Appl Therm

Eng 2017;125:673–85. https://doi.org/10.1016/j.applthermaleng.2017.06.077.
[33] Tian X-X, Kalbasi R, Jahanshahi R, Qi C, Huang H-L, Rostami S. Competition between intermolecular forces of adhesion and cohesion in the presence of graphene nanoparticles: investigation of graphene nanosheets/ethylene glycol surface tension. J Mol Liq 2020:113329. https://doi.org/10.1016/j.molliq.2020.113329.
[34] Li L, Zhai Y, Jin Y, Wang J, Wang H, Ma M. Stability, thermal performance and artificial neural network modeling of viscosity and thermal conductivity of Al2O3-ethylene glycol nanofluids. Powder Technol 2020;363:360–8. https://doi.org/10.1016/j.powtec.2020.01.006.
[35] Yan S-R, Kalbasi R, Nguyen Q, Karimipour A. Sensitivity of adhesive and cohesive intermolecular forces to the incorporation of MWCNTs into liquid paraffin: experimental study and modeling of surface tension. J Mol Liq 2020:113235. https://doi.org/10.1016/j.molliq.2020.113235.
[36] Akhgar A, Toghraie D, Sina N, Afrand M. Developing dissimilar artificial neural networks (ANNs) to prediction the thermal conductivity of MWCNT-TiO2/Water-ethylene glycol hybrid nanofluid. Powder Technol 2019;355:602–10. https://doi.org/10.1016/j.powtec.2019.07.086.
[37] Ma M, Zhai Y, Wang J, Yao P, Wang H. Statistical image analysis of uniformity of hybrid nanofluids and prediction models of thermophysical parameters based on artificial neural network (ANN). Powder Technol 2020;362:257–66. https://doi.org/10.1016/j.powtec.2019.11.098.
[38] Li Y, Kalbasi R, Karimipour A, Sharifpur M, Meyer J. Using of artificial neural networks (ANNs) to predict the rheological behavior of magnesium oxide-water nanofluid in a different volume fraction of nanoparticles, temperatures, and shear rates. Math Methods Appl Sci 2020;n/a. https://doi.org/10.1002/mma.6418.
[39] Ghazvini M, Maddah H, Peymanfar R, Ahmadi MH, Kumar R. Experimental evaluation and artificial neural network modeling of thermal conductivity of water based nanofluid containing magnetic copper nanoparticles. Phys Stat Mech Appl 2020:124127. https://doi.org/10.1016/j.physa.2019.124127.
[40] Hemmat Esfe M, Motallebi SM. Four objective optimization of aluminum nanoparticles/oil, focusing on thermo-physical properties optimization. Powder Technol 2019;356:832–46. https://doi.org/10.1016/j.powtec.2019.08.041.
[41] Yan S-R, Kalbasi R, Nguyen Q, Karimipour A. Rheological behavior of hybrid MWCNTs-TiO2/EG nanofluid: a comprehensive modeling and experimental study. J Mol Liq 2020;308:113058. https://doi.org/10.1016/j.molliq.2020.113058.
[42] Hemmat Esfe M, Kiannejad Amiri M, Bahiraei M. Optimizing thermophysical properties of nanofluids using response surface methodology and particle swarm optimization in a non-dominated sorting genetic algorithm. Journal of the Taiwan Institute of Chemical Engineers 2019;103:7–19. https://doi.org/10.1016/j.jtice.2019.07.009.
[43] Tian X-X, Kalbasi R, Qi C, Karimipour A, Huang H-L. Efficacy of hybrid nano-powder presence on the thermal conductivity of the engine oil: an experimental study. Powder Technol 2020;369:261–9. https://doi.org/10.1016/j.powtec.2020.05.004.
[44] Malvandi A, Heysiattalab S, Ganji DD. Effects of magnetic field strength and direction on anisotropic thermal conductivity of ferrofluids (magnetic nanofluids) at filmwise condensation over a vertical cylinder. Adv Powder Technol 2016;27(4):1539–46. https://doi.org/10.1016/j.apt.2016.05.015.
[45] Li Z, Mohammadali H, Arabkoohsar A, Sheikholeslami M, Shafee A, Ayed MB, et al. Ferrofluid irreversibility and heat transfer simulation inside a permeable space including Lorentz forces. Phys Stat Mech Appl 2019;528:121492. https://doi.org/10.1016/j.physa.2019.121492.
[46] Sheikholeslami M, Arabkoohsar A, Khan I, Shafee A, Li Z. Impact of Lorentz forces on Fe3O4-water ferrofluid entropy and exergy treatment within a permeable semi annulus. J Clean Prod 2019;221:885–98. https://doi.org/10.1016/j.jclepro.2019.02.075.
[47] Gibanov NS, Sheremet MA, Oztop HF, Al-Salem K. Effect of uniform inclined magnetic field on natural convection and entropy generation in an open cavity having a horizontal porous layer saturated with a ferrofluid. Numer Heat Tran, Part A: Applications 2017;72(6):479–94.
[48] Selimefendigil F, Öztop HF. Forced convection of ferrofluids in a vented cavity with a rotating cylinder. Int J Therm Sci 2014;86:258–75.
[49] Selimefendigil F, Öztop HF, Al-Salem K. Natural convection of ferrofluids in partially heated square enclosures. J Magn Magn Mater 2014;372:122–33.
[50] Nguyen Q, Sedeh SN, Toghraie D, Kalbasi R, Karimipour A. Numerical simulation of the ferro-nanofluid flow in a porous ribbed microchannel heat sink: investigation of the first and second laws of thermodynamics with single-phase and two-phase approaches. J Braz Soc Mech Sci Eng 2020;42(9):492. https://doi.org/10.1007/s40430-020-02534-9.
[51] Toghraie D, Alempour SM, Afrand M. Experimental determination of viscosity of water based magnetite nanofluid for application in heating and cooling systems. J Magn Magn Mater 2016;417:243–8. https://doi.org/10.1016/j.jmmm.2016.05.092.
[52] Kalbasi R, Afrand M, Alsarraf J, Tran M-D. Studies on optimum fins number in PCM-based heat sinks. Energy 2019;171:1088–99. https://doi.org/10.1016/j.energy.2019.01.070.
[53] Selimefendigil F, Öztop HF. Numerical study and pod-based prediction of natural convection in a ferrofluids–filled triangular cavity with generalized neural networks. Numer Heat Tran, Part A: Applications 2015;67(10):1136–61.
[54] D. Bahrami, S. Abbasian-Naghneh, A. Karimipour, and A. Karimipour, "Efficacy of injectable rib height on the heat transfer and entropy generation in the microchannel by affecting slip flow," Math Methods Appl Sci, vol. n/a, no. n/a, doi: 10.1002/mma.6728.
[55] Rostami S, Kalbasi R, Talebkeikhah M, Goldanlou AS. Improving the thermal conductivity of ethylene glycol by addition of hybrid nano-materials containing multi-walled carbon nanotubes and titanium dioxide: applicable for cooling and heating. J Therm Anal Calorim 2020. https://doi.org/10.1007/s10973-020-09921-3.